EARTH SCIENCES
RESEARCH JOURNAL
Earth Sci. Res. J. Vol. 28, No. 1 (March, 2024): 3 - 15

UNIVERSIDAD NACIONAL DE COLOMBIA

GEOLOGY

Chemical constraints and tectonic setting of the Ginebra ophiolite complex

Duban Esteban Gomez Gomez[1], Ana Maria Martinez Ardila[2], Juan Carlos Molano Mendoza[1]
1. Departamento de Geociencias, Universidad Nacional de Colombia, Bogotá, Colombia.
E-mail: derochag@unal.edu.co jcmolanom@unal.edu.co
2. Department of Earth and Biological Sciences, Loma Linda University, California, United States.
E-mail: anmartinez@llu.edu

ABSTRACT

The occurrence and types of ophiolites in the Central Cordillera of the Colombian Andes have not been identified in terms of their tectonic settings and geochemical features. Therefore, the study of the tectonic setting and subduction zones in the ophiolites' magmatic evolution becomes a significant issue. The Ginebra Ophiolitic Complex (GOC) is located on the western flank of the Central Cordillera in the Valle del Cauca Department, southwest of Colombia, assigned to the Lower Cretaceous period, as indicated by the contact of the GOC with the Buga Batholith. The GOC is formed by three main lithologies: amphibolite, gabbro, and ultramafic rocks (pyroxenite and peridotite), according to Ossa (2007). The rocks in the Puente Piedra section, located in the northeast of Ginebra municipality, are part of the gabbroic cumulates within the ophiolitic sequence. This sequence comprises interspersed layers of gabbroic cumulates, gabbrodiorites, and diorites; interpreted as a result of crystal accumulation and fractional crystallization processes. The mafic rocks of the GOC are sub-alkaline and correspond to the low potassium (K_2O wt% 0.03-0.06) tholeiitic series. Geochemically, they have SiO_2 wt% ranging from 49 to 61 and an aluminum oxide saturation index of approximately ~0.4 and ~0.8, indicating a metaluminous type. The geochemistry of the studied rocks from Puente Piedra section indicates that the GOC formed through fractional crystallization and accumulation processes from a single magma source. Cluster analysis, used to compare the geochemistry of GOC rocks and the Amaime Complex basalts, suggests a similar magma source, possibly linked to multiple recharge events that underwent fractional crystallization, melt extraction, and accumulation processes. The geochemical parameters are indicative of a suprasubduction zone ophiolite, characterized by a low potassium tholeiitic series affinity, TiO_2 values typically <1.2 wt%, Th enrichment typical of subduction zones, high Pb content, and low values of Ti, Y, Yb, Ta, Nb, Zr, and Hf.

Keywords: Ophiolites; Ginebra Ophiolitic Complex; tectonic setting; suprasubduction zone.

Caracterización geoquímica y evolución tectónica del Complejo Ofiolítico de Ginebra

RESUMEN

La ocurrencia y los tipos de de ofiolitas en la cordillera Central de los Andes colombianos no se han definido claramente en términos de configuración tectónica y características geoquímicas. Por lo tanto, el estudio del entorno tectónico y de las zonas de subducción en la evolución magmática de las ofiolitas se convierte en un tema significativo. El Complejo Ofiolítico de Ginebra (COG) se encuentra en el flanco occidental de la Cordillera Central en el Departamento del Valle del Cauca, suroeste de Colombia, asignado al período Cretácico Inferior, según lo indicado por el contacto del COG con el Batolito de Buga. El COG está formado por tres litologías principales: anfibolita, gabro y rocas ultramáficas (piroxenita y peridotita), de acuerdo con Ossa (2007). Las rocas en la sección de Puente Piedra, ubicada al noreste del municipio de Ginebra, son parte de los cumulados gabroicos dentro de la secuencia ofiolítica. Esta secuencia comprende capas intercaladas de cumulados gabroicos, gabrodioritas y dioritas; interpretadas como resultado de procesos de acumulación de cristales y cristalización fraccionada. Las rocas máficas del COG son subalcalinas y corresponden a la serie toleítica baja en potasio (K_2O wt% 0,03-0,06%). Geoquímicamente, tienen SiO2 wt% que varía de 49 a 61 y un índice de saturación de óxido de aluminio de aproximadamente ~0.4 y ~0.8, indicando un tipo metaluminoso. La geoquímica de las rocas estudiadas de la sección de Puente Piedra indica que el COG se formó a través de procesos de cristalización fraccionada y acumulación a partir de una única fuente de magma. El análisis conjunto de los datos geoquímicos del COG y del Complejo Amaime sugiere una misma fuente de magma, posiblemente vinculada a múltiples eventos de recarga que experimentaron procesos de cristalización fraccionada, extracción de fundido y acumulación. Los parámetros geoquímicos son indicativos de una ofiolita de zona suprasubducción, caracterizada por una afinidad de serie toleítica baja en potasio, valores de TiO_2 típicamente <1.2 wt%, enriquecimiento de Th típico de zonas de subducción, contenido alto de Pb y valores bajos de Ti, Y, Yb, Ta, Nb, Zr y Hf.

Palabras clave: Ofiolitas; Complejo Ofiolítico de Ginebra; configuración tectónica; zona de suprasubducción.

Record
Manuscript received: 08/08/2023
Accepted for publication: 23/04/2024

How to cite this item:
Gómez-Gómez, D. E., Martínez-Ardila, A. M., & Molano-Mendoza, J. C. (2024). Chemical constraints and tectonic setting of the Ginebra ophiolite complex. *Earth Sciences Research Journal, 28*(1), 3-15. https://doi.org/10.15446/esrj.v28n1.110499

ISSN 1794-6190 e-ISSN 2339-3459
https://doi.org/10.15446/esrj.v28n1.110499

1. Introduction

The term "ophiolites" has been used both with a genetic connotation and as a defining feature. It is employed to refer to remnants of ancient oceanic crust, and upper mantle rocks found along continental edges. These remnants consist of a range of rock suites, including felsic, mafic, and ultramafic rocks, which are temporally and spatially associated (Dilek & Furnes, 2014).

As a concept, "ophiolite" rock has experienced a complex evolution, first appearing in Europe in the early nineteenth century. The development of plate tectonics theory marked a turning point for this concept, enabling the beginning of an ophiolite model and facilitating comparisons between ophiolites and oceanic crust. At the first Penrose Conference in 1972, a close relationship between ophiolitic sequences and seafloor environments spreading was proposed. However, in 1973, Miyashiro challenged this model and, based on geochemical interpretations, suggested that the Troodos ophiolite (located in Cyprus) was a product of magmatism within an island arc. The idea was revolutionary and led to a redefinition of ophiolites in suprasubduction zones during the early 1980s (Dilek, 2003; Dilek & Furnes, 2014).

The occurrence and types of ophiolites result from formation processes (tectonic, magmatic, and geochemical) and preservation during the emplacement. Based on these criteria, Dilek and Furnes (2014) proposed that ophiolites would be classified as related and not related to subduction zones in first order. According to Pearce (2014), no subduction-related ophiolites correspond to those that are formed in ocean ridges, plumes, and continental margins. Subduction-related ophiolites include those which were developed in suprasubduction zones and volcanic arcs.

Ophiolites in suprasubduction zones represent the oceanic lithosphere formed in the upper plates extended to the subduction zones, with forearc, back-arc, and nascent arc environment. Forearc ophiolites expose compositional and geochemical variations defined by time: ocean-ridges similar composition (MORB-like) in the oldest ones, to island-arc tholeiites (IAT), and finally boninite-like in those more recent (Dilek & Polat, 2008; Dilek & Thy, 2009; Ishizuka et al., 2014). Magmatic and geochemical evolution in these kinds of rocks is controlled by (1) the partial melting of the crust under the subduction zone and (2) the dehydration melting of elements in a subducted plate under the overlying mantle (Dilek & Furnes, 2014).

The occurrence and types of ophiolites in the Central Cordillera of the Colombian Andes have not been clearly defined. Therefore, an analysis of ophiolite magmatic evolution in extensional environments and subduction zones has become increasingly relevant. Some Colombian ophiolitic clusters have been studied and characterized, such as the Azules Ultramafic Complex, the Pacora's Ophiolitic body, the Bolivar-Valle Mafic-Ultramafic Complex, the Aburra Valley Ophiolite, and the Ginebra Ophiolitic Complex (Espinosa, 1985; Alvarez, 1995; Nivia, 1994, Correa et al., 2005; Restrepo, 2008). The study of ophiolites in the region is necessary to understand Colombia's western lands formation and accretion processes and the geologic evolution of the South American western side during the Cretaceous and Cenozoic.

Despite current studies, a shared understanding of ophiolites petrogenesis has not been reached. Furthermore, some variables have not been studied enough, such as pressure, temperature conditions, and crystallization age. The GOC is a clear example. This study aims to present an evolutive model for the complex. The approach involves, firstly, the petrographic and geochemical characterization of layered gabbros from the ophiolitic sequence. Secondly, the clustered interpretation with geochemical analyses from other levels within the ophiolite sequence of Amaime Complex and Buga Batholith, previously issued by Ossa and Concha (2007) and Villagomez (2011). The study area is locally known as Puente Piedra, twelve kilometers in northeast of Ginebra municipality, southeast of Vereda Regaderos (rural district), on the pathway going to Costa Rica village (Figure 1). Field research, petrographical and geochemical data suggest the mafic-ultramafic rocks in the GOC have been formed in a subduction zone; then, these rocks are classified as ophiolites in a suprasubduction area.

2. Geological setting

The mafic-ultramafic rocks of the GOC with oceanic-like features are located in the western flank of the Colombian Andes' Central Cordillera, to the west of the San Jeronimo fault (Alvarez, 1983). The basement of the region has been reported as a sequence of Cretaceous oceanic rocks (Late Mesozoic) (Aspden & McCourt, 1986; McCourt et al., 1984), which represent an incomplete ophiolitic sequence (Espinosa, 1985). Nivia (1987) stated that a significant part of basic igneous rocks forming the basement in the region are basalts from an oceanic plateau, part of the Western Oceanic Cretaceous Lithospheric Province. Based on geochemical data, Ossa and Concha (2007) proposed that these rocks originated in an oceanic ridge environment and later emplaced along continent edges.

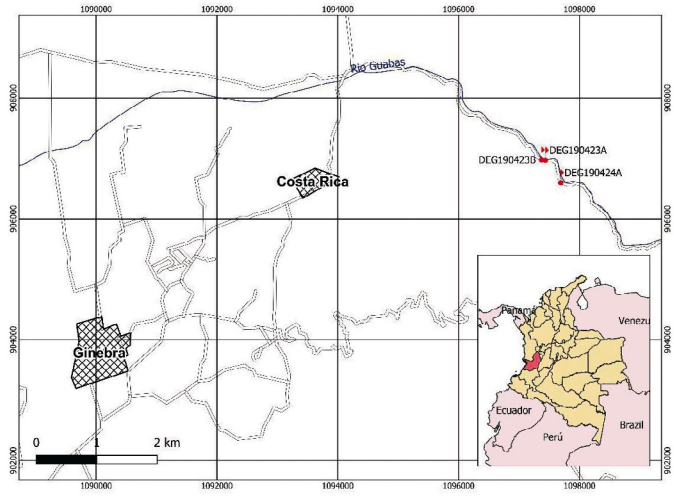

Figure 1. Study area location.

Moreno (2017) recently conducted the petrography and geologic cartography of GOC gabbros exposed in the Ginebra municipality. This work is a continuation of the research developed by Moreno, including, from west to east, the Ginebra Ophiolitic Complex, Buga Batholith, and Amaime Complex (Figure 2). Porphyritic bodies with no-mapping dimensions are observed in the study area, but they represent different and younger geological events (Rodriguez, 2012). Underlying this sequence is reported the Cenozoic La Paila Formation.

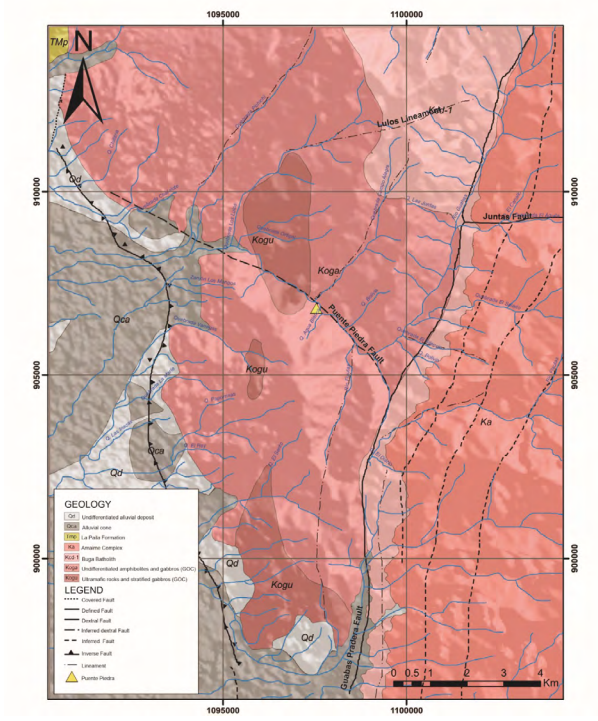

Figure 2. Geological and structural cartography of the Puente de Piedra section region. Modified from Rodriguez (2012).

Amaime Complex (Ka). Previous studies have used the term "Amaime Formation" (McCourt et al., 1984; Nivia, 1987; Nivia, 2001). However, according to the American Stratigraphic Code guidelines for denotation and terminology of lithodemic units, the authors will use Amaime Complex to reference to this volcanic complex. The Amaime Complex corresponds to a green-dark colored tholeiitic basaltic series, which is hyaline to holocrystalline, and exhibits a subophitic texture (McCourt et al., 1984). It consists of pillow lavas and minor sedimentary layers exposed in the western flank of the Central Cordillera, west of the Cauca-Almaguer Fault (Lopez, 2006; McCourt et al., 1984). Locally, the Amaime Complex borders the west with the Guabas-Pradera Fault, and in contact with the GOC and the Buga Batholith (Figure 2).

The age of the Amaime Complex can be established based on the relative temporal relationship of the basalts. During the formation of the basalts, accretion occurred at the continent edge; then, the basalts were intruded by the Buga Batholith (Rodriguez, 2012). Brook (1984) suggested a 94±4 Ma for the Buga Batholith with a calculation based on the Rb/Sr method applied in biotite and hornblende. Furthermore, Villagomez et al. (2011) reported two zircon U-Pb ages of approximately 90 ma for the same unit. Following this, Moreno (2017) proposed that the age of the Amaime Complex is older than 100 Ma, while Rodriguez (2012) suggested an origin in the Late Jurassic to Early Cretaceous.

Ginebra Ophiolitic Complex (Kog). The GOC was defined by Espinosa (1985), as a block of mafic and ultramafic rocks. This block exhibits an enlarged geometry in a N-S direction, with an average length of 40 km and a width of 8 km. It is bounded by faults on both flanks. To the east, it is delimited by the Guabas-Pradera Fault, where it comes into contact with the Amaime Complex. To the west, its delimited by the Palmira-Buga fault, making its contact with the Miocene sedimentary units of the La Paila Formation (Figure 2).

Three main groups of rocks form the GOC: amphibolites, gabbros, and pyroxenites and peridotites. The amphibolites represent the most significant percentage of the GOC; fine to medium-grain texture, made of hornblende, plagioclase, quartz, opaque minerals (especially ilmenite), and apatite and epidote in a lower proportion. The amphibolites originated from metamorphism of microgabbros and basalts. Gabbros in the cumulus zone are layered, sub-alkaline, and they are part of the tholeiitic series low in potassium (Nivia, 1987; Ossa & Concha, 2007).

Ossa and Concha (2007) reported that the magmas responsible for the mafic and ultramafic rocks originated from a mid-oceanic ridge, specifically the N segment of the upper mantle (MOR-N). In addition, Ossa and Concha proposed that these magmas, along with the Amaime Complex, appear to form an incomplete ophiolitic sequence which may be part of an older geologic basement. This sequence differs from the Western Oceanic Cretaceous Lithospheric Province defined by Nivia (1987).

Rodriguez (2012) suggested that, based on the contact relationships (McCourt et al., 1984) and calculated ages established for the Buga Batholith, which range from 90-96 Ma (Brito et al., 2010; Villagomez et al., 2011), the minimum age of the GOC is younger than the Early Cretaceous. On the other hand, Nivia et al. (2017) proposed that the Buga Batholith represents an intrusive-syntectonic body within the GOC. This idea is supported by ^{40}Ar-^{39}Ar ages for GOC rocks, revealing a 140.28±3.12 Ma age (in clinopyroxene) for a gabbronorite, interpreted as the crystallization age, and an age of 90.84±0.78 Ma (in hornblende) for an amphibolite, interpreted as the reworking age of the GOC due to the syntectonic crystallization of the Buga Batholith.

Buga Batholith (Kcd-1). The Buga Batholith as described by Aspden et al. in 1987, is a calc-alkaline granitoid in the Buga, San Pedro, and Tulua municipalities. This batholith exhibits a composition ranging from hornblendic to tonalitic quartz diorite, with hornblendic diorite present at its contacts, particularly along the western boundary where the batholith is in contact with metabasalts of the GOC (Nivia, 2001).

The Buga Batholith intrudes the GOC in the northern region, forming a roof pendant structure. This is further supported by the presence of veins and dikes in contact areas where the batholith intrudes the tholeiites of the Amaime Complex, suggesting a clear intrusive relationship with the Amaime Complex. Additionally, a significant area of the contact between these two units correspond to a faulted contact, and the western boundary of the Buga Batholith is defined by the Guabas-Pradera Fault (Figure 2) (Nivia, 2001).

The age of this batholith has been a subject of various interpretations based on different dating methods. Touissant and Restrepo (1978) reported a K/Ar age of 113±10 Ma for hornblende; Brook (1984) obtained a Rb/Sr age of 99±4Ma in biotite; Brito et al. (2010) calculated a U-Pb (SHRIMP) age 96.79 Ma. in zircon; and Villagomez et al. (2011) found a range of U-Pb zircon ages from 90.6±1.3 to 92.1±0.8 Ma. Nivia et al. (2017) suggests the existence of two plutons of different ages in the mapped area known as the Buga Batholith, with average ages of 88±1.64 Ma and 69±1.41 Ma using the U-Pb method on zircon. As a result, the areas where samples of 69 Ma age were collected were separated as an independent unit.

Porphyritic bodies. In 2012, Rodriguez presented the first assessment of the porphyritic bodies within the region and classified these as dacitic porphyries. These bodies intrude Buga Batholith and GOC and ranging in width from two to ten meters. However, they are not mappable on a 1:25000 scale. The age of these porphyritic bodies has been determined through U-Pb LA-ICP-MS dating yielding an age range between 70.61 and 65.4 Ma. (Brito et al., 2010).

La Paila Formation (TMp). This formation initially proposed by Keizer in 1954 is characterized as a conglomerate body with interbedded dacitic tuff layers. Subsequently, Nelson in 1957 divided the formation into two distinct units. The lower unit spans approximately 200 m and is primarily composed of dacitic tuffs, while the upper unit consists of a clastic sequence, predominantly conglomeratic in nature. The thickness of the sequence varies from 400 to 600 m. This unit exhibit a faulted contact with the GOC in the east, and it is partially covered by alluvial and colluvial deposits towards the west (Rodriguez, 2012) (Figure 2). The age of the La Paila Formation has been a subject of debate among researchers. According to palynological data provided by Van der Hammen in 1958 and Schwin in 1969, the formation is believed to be of Miocene age. However, McCourt, in 1984, suggested that this unit might be older, likely dating back to the Oligocene period. McCourt's perspective also links it partially to the Cauca Group and Amaga Formation.

3. Methodology

Field observations

In the Puente Piedra section, located in Ginebra municipality, Valle del Cauca (Figure 1), a lithologic and detailed sampling as well as magnetic susceptibility measurements were conducted for this study. An SM30 ZH susceptibility meter was employed to the measurements.

Petrography

A total of eight polished thin sections were analyzed from the GOC rocks, collected in the Puente Piedra area. Analyses were performed with a Primotech microscope (built-in cam), and each sample was classified following Le Bas & Streckeisen (1991) based on a 300-500 points during point counting according to mineralogic variations and textural characteristics. The complete list of these polished thin sections, their locations, textural classifications, and mineralogy is documented in Annex 1.

Whole Rock geochemistry

Whole-rock analyses were conducted on seven gabbro rocks from the GOC, including both major and trace elements. The analyses were carried out at the ALS Chemex laboratory, located in Medellin, Colombia, utilizing coupled plasma mass spectrometry (ICP-MS) and coupled plasma atomic emission spectroscopy (ICP-AES). In Annex 2, information of used standards and detection limits for every element can be found.

The selected samples for geochemical analyses were homogenous, with no visible inclusions or evidence of hydrothermal alterations. Additionally, this study included geochemical data published by Ossa and Concha (2007), who analyzed 19 samples from the GOC and one from the Amaime Complex. Furthermore, data reported by Villagomez (2011), from three samples of the Amaime Complex and two samples from the Buga Batholith were used. The GCDkit 5.0 software (Janoušek et al., 2006) was employed for the creation and visualization of geochemical diagrams. The plots generated included: alteration index, magmatic series characterization, geochemical classification, Harker diagrams, and tectonic discriminant diagrams proposed by Pearce (2008) and Pearce (1982). SiO_2 was chosen as the normalizing element for both major and trace element variation diagrams. For Rare Earth Elements (REE), plotting

values of primitive mantle were selected according to McDonough and Sun (1995). Results of normative mineral calculations (CIPW Norm) and analyses standardized to 100% (free of H_2O+, H_2O-, and CO_2) are listed in Annex 3.

4. Results

Field observations

The studied segment in the ophiolitic sequence is composed of intermittent felsic and mafic layering with similar orders of magnitude to one another -from millimetric to 30 cm width (Figure 3). The felsic layers exhibit equigranular textures with hypidiomorphic fine crystals (0.05-1 mm) composed of quartz, plagioclase, and hornblende. The mafic layers present mesocratic, equigranular-phaneritic textures, composed of fine to very-fine (<0.03-1 mm) crystals of plagioclase and pyroxene. The magnetic susceptibility shows a constant proportionality with the color index of the bands ranging from 2 to 8 for leucocratic bands and from 25 to 39 for mesocratic and melanocratic bands.

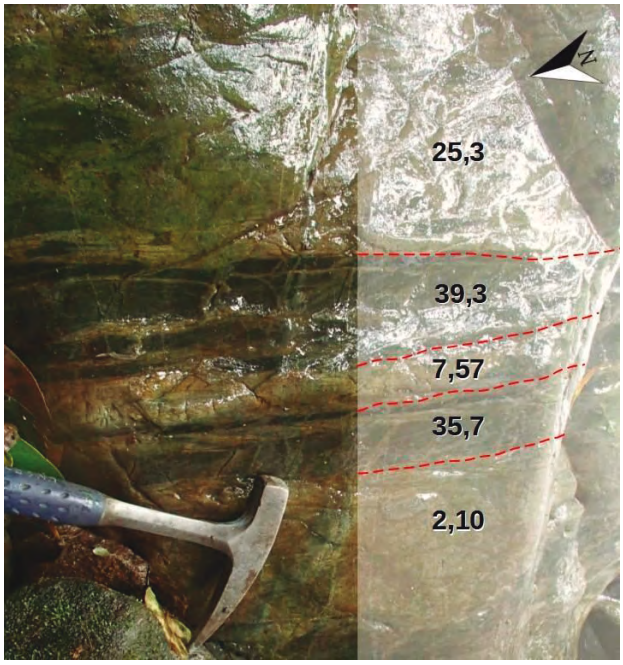

Figure 3. Felsic and mafic interbedding at the gabbros band level of the GOC ophiolitic sequence. Values correspond to the magnetic susceptibility, which is higher in the mafic bands.

Petrography and rock compositions

Petrographic analyses confirms that the studied section of the GOC is formed by isotropic gabbros, cumulate gabbros, gabbrodiorites, and diorites that were hydrothermally altered or deformed. Modal analyses and compositional classifications are presented in Figure 4.

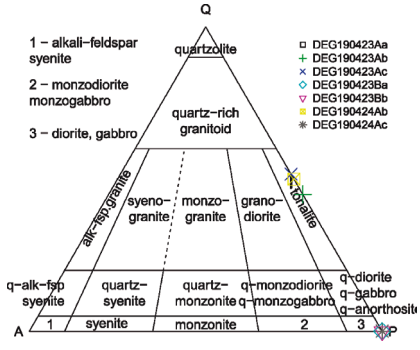

Figure 4. QAP diagram applied to gabbro rocks in the Ginebra Ophiolitic Complex at the Puente de Piedra section

Isotropic gabbros

The isotropic gabbros are holocrystalline, equigranular, fine to medium crystal size with anhedral to subhedral crystals, composed by plagioclase, clinopyroxene, orthopyroxene, hornblende, magnetite, and ilmenite. These rocks are moderately affected by hydrothermal alteration; the secondary minerals formed as result of hydrothermal alteration are hornblende, epidote, and chlorite (Figure 5a).

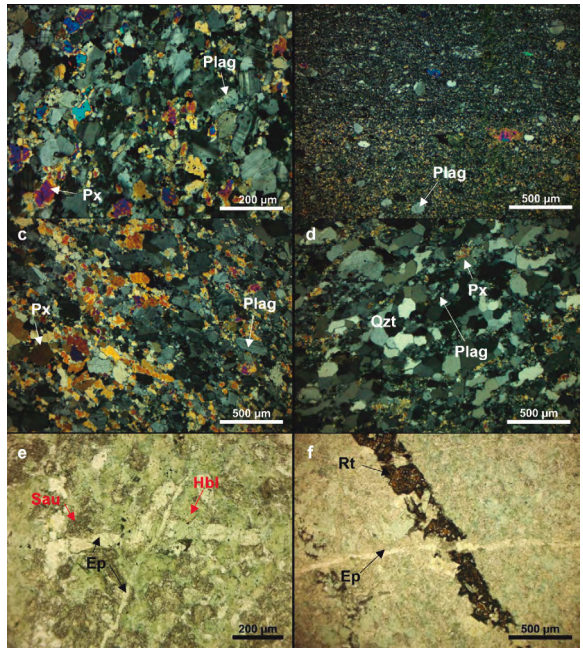

Figure 5. Petrographic observations of characterized rocks in the Puente de Piedra section. a) Isotropic gabbro; b) cumulate gabbros; c) gabbrodiorite; d) diorite; e) hornblende and saussurite formed through hydrothermal alteration of pyroxenes and plagioclases, respectively; f) rutile vein (NW-SE) cut by an epidote vein (W-E). Plagioclase (Plag), pyroxene (Px), quartz (Qzt), saussurite (Sau), hornblende (Hbl), epidote (Ep), rutile (Rt).

Cumulate Gabbros

These rocks exhibit an oriented texture characterized by both broken and thick crystals, surrounded by finely milled material. Multiple twinnings in the plagioclase crystals appear deformed in flame-like shapes. The cumulates are formed dominantly by plagioclase, orthopyroxene, clinopyroxene, and magnetite. When observed using mesoscopic and microscopic techniques cumulate textures are identified, marked by variations in the proportions of minerals (plagioclase/pyroxene), changes in crystal size, and differences in magnetite content.

Gabbrodiorites

The gabbrodiorites exhibit mineral fabrics, holocrystalline and equigranular textures with fine to very fine size anhedral crystals. These rocks are primarily composed by plagioclase and clinopyroxene with smaller amounts of quartz subgrains formed during a deformation stage (Figure 5c).

Diorites

These rocks exhibit holocrystalline inequigranular texture with fine anhedral crystals formed by plagioclase, clinopyroxene, and quartz. The quartz crystals show mosaic texture due to deformation (Figure 5d). In some layers, abundance of pyroxene and ilmenite is observed. There are zones characterized by intense hydrothermal alteration with hornblende and chlorite modifying the pyroxene crystals (main clinopyroxene) and saussurite scattered over plagioclase crystals (Figure 5e). Some clusters of small veins were identified and characterized as follows: (1) amphibole (with magnetite or ilmenite);

(2) epidote-rutile; (3) chlorite; (4) amphibole and epidote (with ilmenite and magnetite); and (5) zoisite-clinozoisite-epidote (Figure 5f).

Geochemical data

The rocks in the studied section are part of a tholeiitic series with a high concentration of SiO_2, varying from 52 to 62 wt% (Figure 6), and an alumina saturation index ranging from ~0.4 to ~0,8. These values indicate that the rocks from the GOC, the Amaime Complex, and Buga Batholith correspond to metaluminous igneous rocks (Figure 7). The differentiation of the three compositional groups within the ophiolitic sequence, gabbros, gabbrodiorites, and diorites (as shown in Figure 8), is based on the SiO_2 vs. alkali ratio in the rocks.

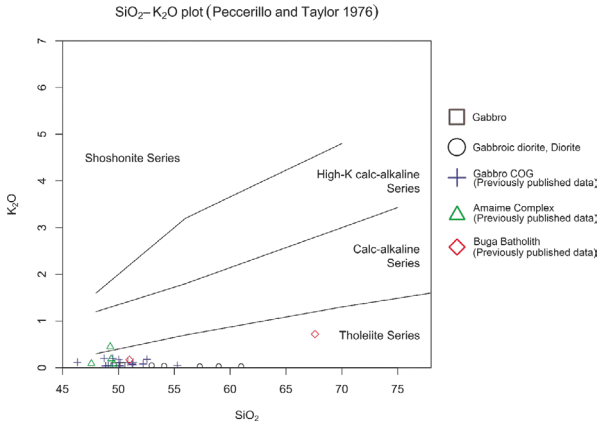

Figure 6. K_2O vs. SiO_2 chart suggested by Peccerillo and Taylor (1976). These conventions apply to all of the charts listed below.

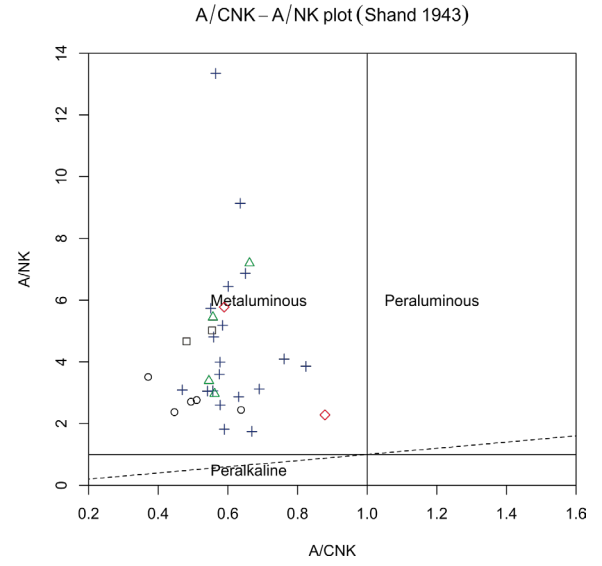

Figure 7. A/NK vs. A/CNK chart suggested by Shand (1943) to determine Al_2O_3 saturation.

The variation in major oxides with respect to the SiO_2 content in the analyzed rocks reveals two different trends: (a) a positive collinear trend for TiO_2 and Na_2O, and a negative trend for K_2O, Al_2O_3, FeOt, and CaO in the Puente Piedra section. (b) Conversely, gabbros collected from La Honda (Ginebra municipality) and El Diamante (Buga's municipality) locations exhibits a linear with a steep vertical slope concerning the major oxides in relation to SiO_2 (ranging from 46 to 55 wt%), with a wide range of values for K_2O and FeOt, and a similar range of values for MgO, CaO, Al_2O_3, and TiO_2 when compared to the samples from the Puente Piedra (Figure 9).

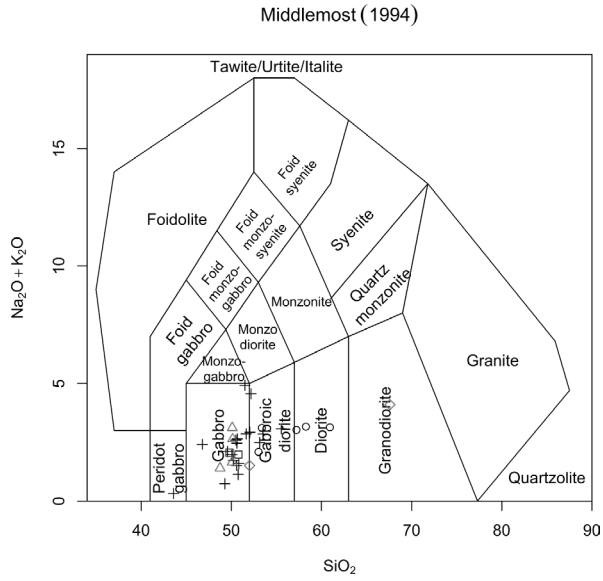

Figure 8. TAS chart for geochemical classification of rocks from the GOC, Complejo Amaime and Buga Batholith.

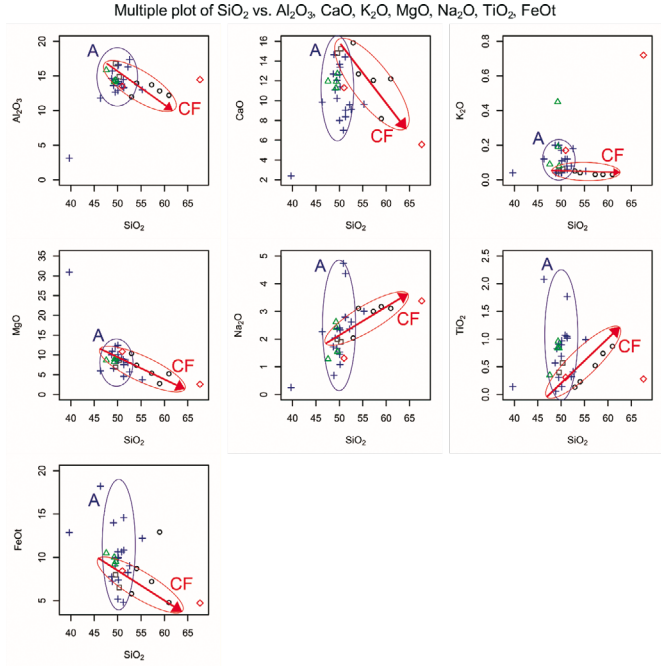

Figure 9. Harker vs. SiO_2 variation diagram for major oxides for the GOC, the Amaime complex, and the Buga Batholith. A: Accumulation, CF: Fractioned Crystallization.

Regarding TiO_2, the gabbro samples from the GOC generally exhibit concentrations of less than 1.2 wt%, except for two samples analyzed by Ossa and Concha (2007). A similar range is observed in the results obtained by Villagomez (2011) and those of Ossa and Concha (2007) for the basaltic rocks in the Amaime Complex (Figure 10).

In analyzing the behavior of trace elements in the GOC (Figure 11) concerning their variation relative to SiO_2 content, two primary trends were observed, consistent with the patterns described for major oxides. Within the Puente Piedra section, rocks display a linear increase with a positive slope for elements such as lanthanum, cerium, yttrium, and zirconium, while showing

a slight negative slope for barium and strontium. In contrast, rocks from La Honda and El Diamante, as reported by Ossa and Concha in 2007, exhibit a vertical trend over a narrow SiO_2 content range.

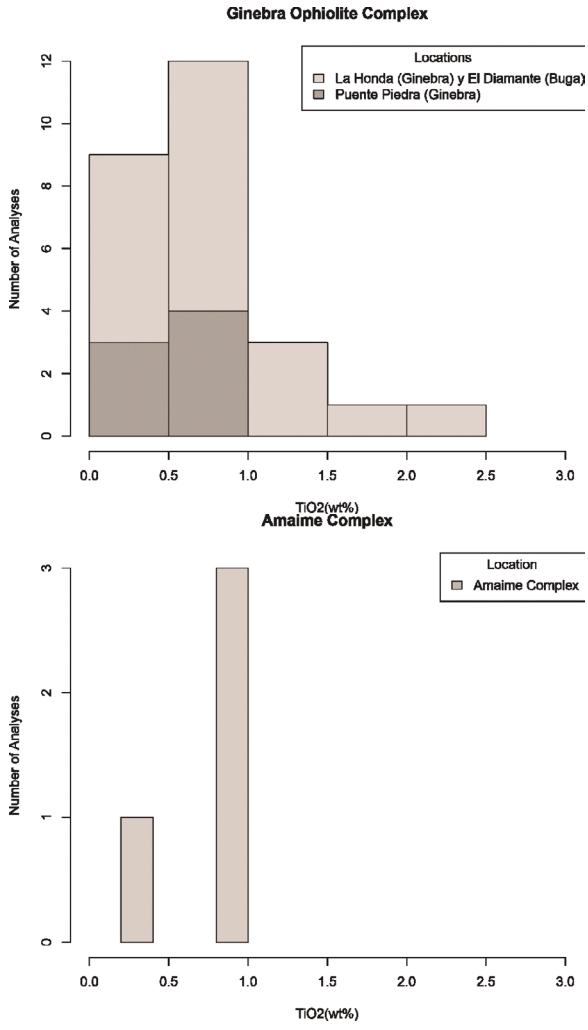

Figure 10. Histogram displaying the weight percentage of TiO_2 (wt%) content at two locations: a) GOC and b) Amaime Complex.

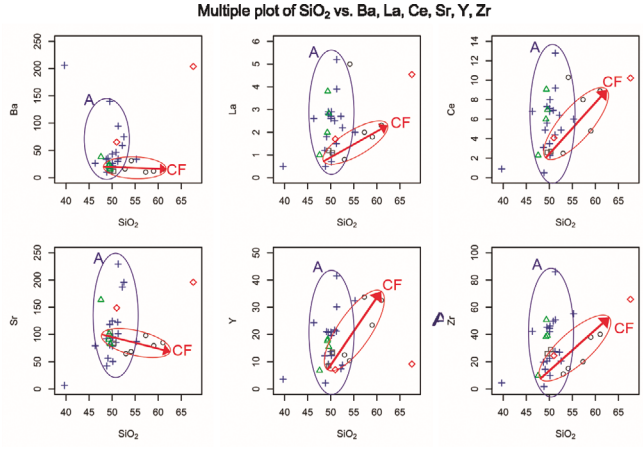

Figure 11. Harker vs. SiO_2 variation diagram for trace elements of rocks from the GOC, the Amaime Complex, and the Buga Batholith. A: Accumulation, CF: Fractioned Crystallization.

In general, the rocks from the GOC, Amaime Complex, and Buga Batholith exhibit enriched concentrations of large-ion lithophile elements (LILE: Cs, Rb, Ba, Th, K, Sr, and Pb) and slightly depleted concentrations of high-field strength elements (HFSE: Nb, Ta, Hf, Zr, Ti) with respect to normal mid-ocean ridge basalts (N-MORB) (Figure 12). It is important to mention the similarity in patterns between the gabbros from the GOC, the basalts from Amaime Complex, and the granitic rocks from the Buga Batholith.

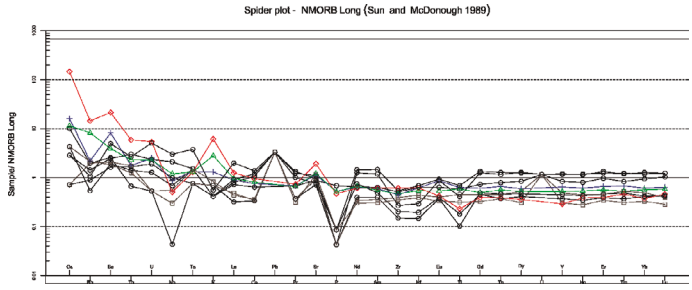

Figure 12. Normalized trace elements with respect to N-MORB for the GOC, Amaime Complex, and Buga Batholith.

Considering the behavior of the rare-earth elements (REE) as depicted in the multi-elemental diagram (Figure 13), distinct trends for each lithologic unit can be identified. Rocks from the Amaime Complex display a flattened-shaped pattern, enriched in a four-factor ratio concerning the the primitive mantle. Rocks from the Buga Batholith show a negative slope, indicating a relative depletion of heavy rare-earth elements (HREE). Finally, the GOC rocks show a flattened-shaped pattern but are depleted in light rare-earth elements (LREE). Within this unit, the more differentiated lithologies, such as gabbrodiorites and diorites, are more enriched in rare-earth elements than the less differentiated lithologies, suchs as gabbros. Additionally, the gabbros of the GOC display moderate positive Eu anomalies, while the gabbrodiorites and diorites present moderate-to-heavy negative Eu anomalies.

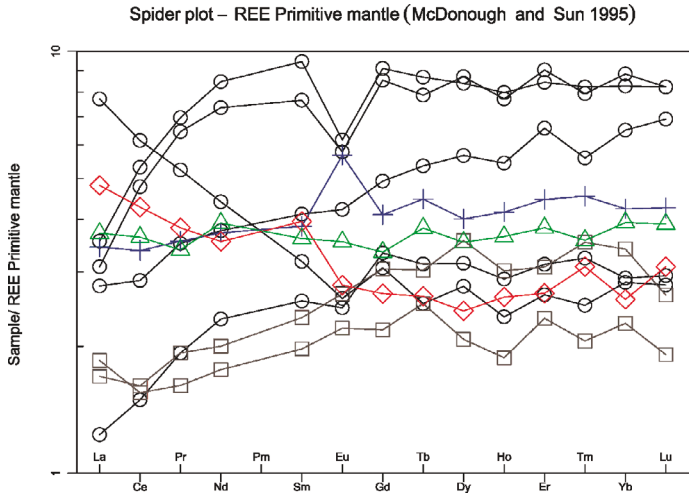

Figure 13. Normalized REE elements with respect to the primitive crust of rocks from the GOC, Amaime Complex, and Buga Batholith.

5. Discussion

The field study observations and the petrography and geochemistry results have allowed authors to characterize the Puente Piedra sections rocks as part of the cumulate gabbros level in the ophiolitic sequence with interbedding of gabbros, gabbrodiorites, and diorites upon fractional crystallization,deformation, and hydrothermal alterations.

The GOC rocks have a sub-alkaline character. They are part of the tholeiitic sequence with a relative enrichment of FeOt with respect to MgO; and display a tholeiitic trend low in potassium. When examining the geochemical behavior of major and trace elements (Figures 9 and 11) for the GOC, two

distinct processes governing crystallization become evident. Firstly, in the Puente Piedra section the formation of gabbro was influenced by a fractional crystallization process dominated by a single magma source. The dispersion of data for K_2O and Na_2O is attributed to the geochemical alterations in the analyzed rocks. The trend observed in Al_2O_3, FeOt, MgO, and CaO indicates a typical behavior, as these elements participate in the fractional crystallization of olivine, orthopyroxene, clinopyroxene, plagioclase, and hornblende. Conversely, in La Honda and El Diamante locations crystallization appears to have been controlled by extraction and accumulation processes, as evident from the wide range of values found in CaO (2.39-14.65 wt%), FeOt (5.34-20.25 wt%), MgO (3.74-30.93 wt%), Na_2O (0.25-4.74 wt%), La (0.50-5.20 wt ppm), Ce (0.50-12.80 wt ppm), Sr (6.60-229.20 wt ppm), Y (2.20-41.50 wt ppm), and Zr (1.80-86.00) for restricted values of SiO_2 (46.33-55.27 wt%).

The geochemistry of the Puente Piedra section, as well as that of La Honda and El Diamante locations, displays a chemical signature consistent with the the upper mantle (N-MORB), as reported by Ossa and Concha in 2007. Certain, distinctive characteristics allow us to suggest that the rocks from the GOC were formed in a tectonic setting associated with subduction rather than an oceanic ridge, challenging previous models.

The TiO_2 content in the GOC samples fall within the range of 0.06-2.8 wt% with a mode of 0.9 wt%, while in the Amaime Complex it varies within the range of 0.35 to 0.93 wt%, with a mode close to 0.84 wt%. These TiO_2 content levels are consistent with those observed in basalts from modern subduction zones such as the Mariana and Tonga subduction zones (Metcalf & Shervais, 2008).

The content of trace elements in rocks and minerals is influenced by the tectonic setting and conditions controlling magma generation (Pearce, 2014). Rocks formed in island arcs, often exhibit selective enrichment in certain elements, particularly the LILE elements derived from the subducted slab (strontium, potassium, rubidium, barium, Th ± Ce ± Sm ± P); and depletion of HFSE (tantalum, niobium, hafnium, zirconium, titanium, yttrium, ytterbium) as a result of the hydrated melting conditions (Metcalf & Shervais, 2008; Pearce et al., 1984). These enrichment and depletion features were observed in the GOC, the Amaime Complex, and in the Buga Batholith (Figure 12). Notably, these patterns exhibit remarkable similarities across the three geologic units. The similarities are significant, particularly because the Buga Batholith has been classified as part of an island arc based on its calc-alkaline affinity and characteristic magmatic signature from the mantle within the suprasubduction zone, as documented by Villagomez (2010) and Nivia et al. (2019).

Based on the geochemical analyses of the cumulate gabbros at the Puente Piedra section and the data obtained from the Amaime Complex and the GOC, it can be concluded that these units share a genetic relationship and collectively represent an ophiolitic sequence and a potential suprasubduction tectonic environment during its formation. This sequence is distinct from the Western Cretaceous-Oceanic Lithospheric Province, as reported by Ossa and Concha in 2007.

Tectonic differentiation

Basaltic rocks from various ophiolitic sequences around the world have played a significant role in distinguishing the formation environments of these sequences, as their geochemistry is indicative of the tectonic processes involved (Pearce, 2008). Thus, by examining the geochemical data compiled in the studies by Ossa & Concha (2007) and Villagomez (2011), the following observations supported the model that the GOC is a suprasubduction zone ophiolite type.

The tectonic discrimination was conducted using the criteria established by Yang et al. (2014) and Dilek & Furnes (2014), which, in turn, rely on the geochemical characteristics outlined by Pearce (2008). The Nb/Yb vs. Th/Yb diagrams are used to compare incompatible elements and can tectonically discriminate mafic rocks (Figure 14).

The Nb/Yb vs. Th/Yb diagram shows interactions between magma and the continental crust in two ways: by indicating either crustal contamination or the presence of a subduction component (Pearce & Peate, 1995). In the diagram, MORB and Ocean Island Basalt (OIB) materials form a diagonal shape with average values for N-MORB, E-MORB, and OIB at the center. Consequently, magmas interacting with the continental crust will exhibit higher Th/Yb values. Some samples from the GOC and the Amaime Complex exhibit thorium enrichment, which is consistent to the enriched values found in subduction zones (Pearce, 2008; Yang et al., 2014).

TiO_2 values for the GOC and Amaime Complex are within the average range, aligning with the statistical distribution of rocks formed in arc environments (Metcalf & Shervais, 2008). The behavior of trace elements in rocks from these units, characterized by LILE enrichment, non-enrichment, and even depletion of HFSE and REE compared to N-MORB, aligns with the pattern of rocks formed in suprasubduction environments, such as the Trinity ophiolite and Troodos ophiolite (Pearce et al., 1984; Metcalf and Shervais, 2008).

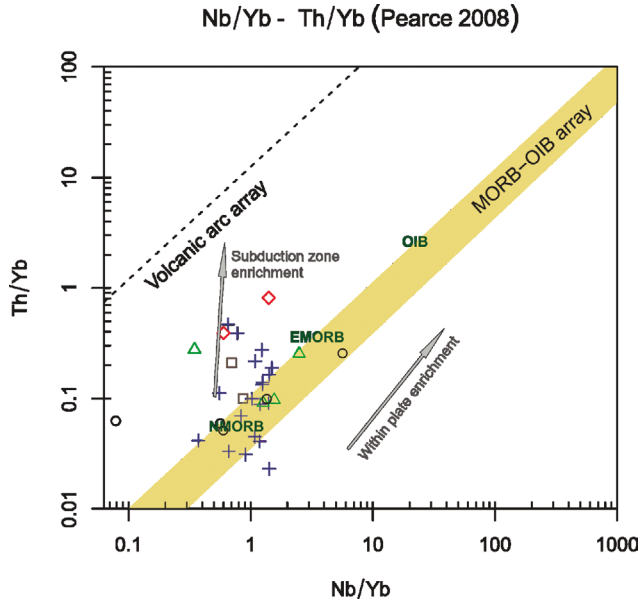

Figure 14. Tectonic Th-Nb differentiation chart applied for the rocks from the GOC, the Amaime Complex, and the Buga Batholith. Modified from Pearce (2008).

Suprasubduction basalts are geochemically characterized by low amounts of Ti, Y, Yb, Ta, Nb, Zr, and Hf. These trace elements exhibit values that are either lower or closer to the average N-MORB values because no enrichment of these trace elements occur in subduction zones. This characteristic would be a consequence of hydrated conditions during partial melting, causing the melting of a refractory crust, increasing the degree of partial melting, or stabilizing minor oxides in the residual molten phase (Pearce et al., 1984). The described patterns were observed in tholeiitic rocks from the Amaime Complex (Figure 15), and the behavior and values of these rocks observed in the N-MORB normalized plot were similar to the South Sandwich basalts, described as tholeiitic basalts from a suprasubduction zone (Ozcan et al., 2020).

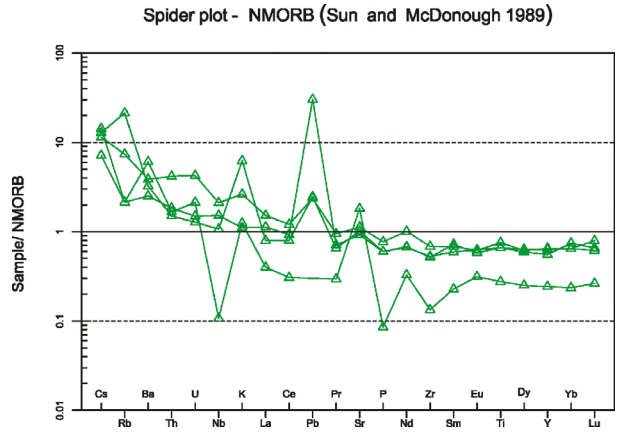

Figure 15. Multi-elements N-MORB normalized chart applied to geochemical data from the Amaime Complex published by Villagomez (2011).

Basalts from the suprasubduction zone exhibit lower Yb in comparison to MORB basalts. This observation is evident in the Cr-Y diagram (Figure 16), where the basalts from the Mariana Trench fall within the zones of island arc tholeiitic basalts (IAT) on the right and, as suggested by Pearce et al. (1984), on the left, representing the analogous elements for suprasubduction ophiolites. Notably, two basalt samples from the Amaime Complex share similarities with the IAT zones, while all three samples show resemblances to rocks from the Mariana trench.

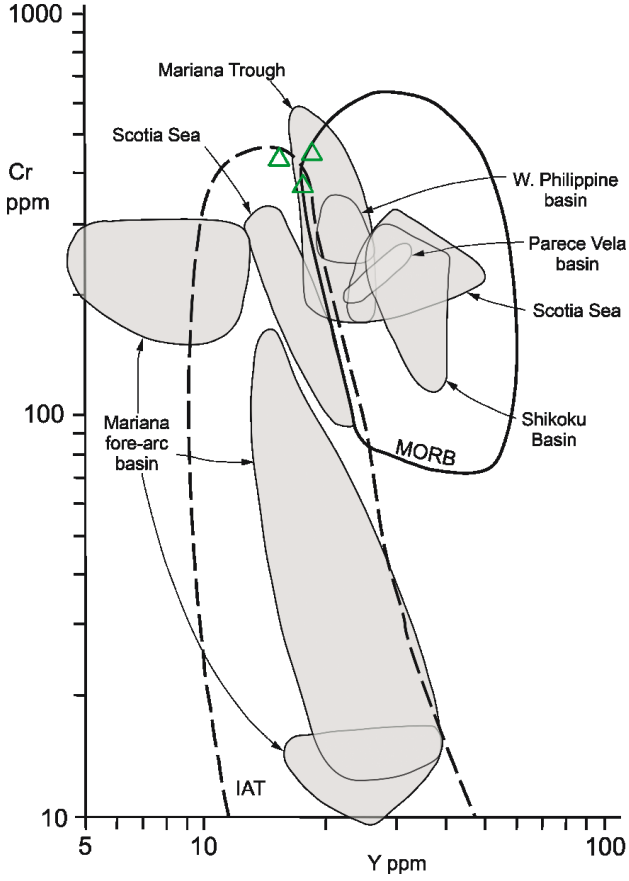

Figure 16. Cr-Y differentiation chart by Pearce (1982) deploying the separation of the oceanic ridge basalts from the Island Arc tholeiitic rocks (IAT) and applied to basaltic rocks from the Amaime Complex. (Pearce, 1984)

The authors wish to to emphasize the importance of including geochemistry and single mineral chemistry in future GOC research studies for data analysis and tectonic environment discrimination, following the methodology proposed by Gervila et al. (2005) and Proenza (2004). This recommendation aims to validate the formation model of the GOC within a suprasubduction tectonic setting, as proposed in this study. Additionally, the authors look forward to future studies and contributions on other petrogenetic variables, such as the pressure, temperature, and the crystallization age of the GOC.

References

Alvarez A., J. (1983). Geología de la Cordillera Central y el occidente colombiano y petroquímica de los intrusivos granitoides mesocenozoícos. *Boletín Geológico,* 26(2), 175.

Álvarez, A., J. (1995). Geología del Complejo Ofiolítico de Pácora y secuencias relacionadas a Arco de Islas (Complejo Quebradagrande), Colombia. *Boletín Geológico,* 35(1), 5-49

Aspden, J. A., & McCourt, W. J. (1986). Mesozoic oceanic terrane in the central Andes of Colombia. *Geology,* 14(5), 415–418. https://doi.org/10.1130/0091-7613(1986)14<415:MOTITC>2.0.CO;2

Aspden, J. A., McCourt, W. J., & Brook, M. (1987). Geometrical control of subduction-related magmatism: the Mesozoic and Cenozoic plutonic history of Western Colombia. *Journal of the Geological Society*, 144(6), 893–905. https://doi.org/10.1144/gsjgs.144.6.0893

Brito, R., Molano, J. C., Rodriguez, B., Dorado, C. (2010). *U-Pb LA-ICPMS dating of the Buga Batolith and associated Porphyry dykes of the Ginebra Ofiolite-Westernmost Central Cordillera-Colombia*. VII South American Symposium on Isotope Geology, Vol. 2, Brasília, Brasil, pp. 252-256.

Brook, M. (1984). New radiometric age data from SW Colombia. Cali: Ingeominas–Mision Britanica (British Geological Survey), Report, 10.

Correa, A. M., Martens, U., Restrepo, J. J., Ordóñez-Carmona, O., & Pimentel, M. M. (2005). Subdivisión de las metamorfitas básicas de los alrededores de Medellín Cordillera Central de Colombia. Revista de la Academia Colombiana de Ciencias Exactas, Físicas y Naturales, 29(112), 325-343.

Dilek, Y. (2003). Ophiolite concept and its evolution. *Geological Society of America*, 373, 1–16. https://doi.org/10.1130/0-8137-2373-6.1

Dilek, Y., & Furnes, H. (2014). Ophiolites and their origins. *Elements*, 10, 93–100. https://doi.org/10.2113/GSELEMENTS.10.2.93

Dilek, Y., & Polat, A. (2008). Suprasubduction zone ophiolites and Archean tectonics. *Geology,* 36(5), 431–432. https://doi.org/10.1130/Focus052008.1

Dilek, Y., & Thy, P. (2009). Island arc tholeiite to boninitic melt evolution of the Cretaceous Kizildag (Turkey) ophiolite: Model for multi-stage early arc–forearc magmatism in Tethyan subduction factories. *Lithos,* 113(1), 68–87. https://doi.org/https://doi.org/10.1016/j.lithos.2009.05.044

Espinosa, A. (1985). *El macizo de Ginebra(V), una nueva secuencia ofiolitica sobre el flanco occidental de la Cordillera Central; Le massif de Ginebra(V), une nouvelle séquence ophiolitique sur le flanc occidental de la Cordillère centrale.* Congreso Latinoamericano de Geología, 6 (pp. 46–57). Ingeominas.

Gervilla, F., Proenza, J. A., Frei, R., Gonzalez-Jimenez, J. M., Garrido, C. J., Melgarejo, J. C., ... & Lavaut, W. (2005). Distribution of platinum-group elements and Os isotopes in chromite ores from Mayarí-Baracoa Ophiolitic Belt (eastern Cuba). *Contributions to Mineralogy and Petrology*, 150(6), 589-607.

Ishizuka, O., Tani, K., & Reagan, M. K. (2014). Izu-Bonin-Mariana Forearc Crust as a Modern Ophiolite Analogue. *Elements,* 10(2), 115–120. https://doi.org/10.2113/gselements.10.2.115

Janoušek, V., Farrow, C. M., & Erban, V. (2006). Interpretation of whole-rock geochemical data in igneous geochemistry: introducing Geochemical Data Toolkit (GCDkit). *Journal of Petrology,* 47(6), 1255–1259. https://doi.org/10.1093/petrology/egl013

Keizer, J. (1954). *Contribución al conocimiento de la Cordillera Occidental. La geología del flanco oriental de la Cordillera Occidental en la región de San Antonio, Municipio de Jamundí, Valle del Cauca*. Servicio Geológico Nacional. Bogotá.

Le Bas, M. J., & Streckeisen, A. L. (1991). The IUGS systematics of igneous rocks. *Journal of the Geological Society*, 148(5), 825–833.

López, M. C. (2006). *Análisis de deformación tectónica en los pie de montes de las cordilleras Central y Occidental, Valle del Cauca, Colombia-Contribuciones Paleosísmicas.* Universidad Eafit, Medellín, Colombia.

McCourt, W. J., Aspden, J. A., & Brook, M. (1984). New geological and geochronological data from the Colombian Andes: continental growth by multiple accretion. *Journal of the Geological Society*, 141(5), 831 LP – 845. https://doi.org/10.1144/gsjgs.141.5.0831

McDonough, W. F., & Sun, S. S. (1995). The composition of the Earth. *Chemical geology*, *120*(3-4), 223-253. https://doi.org/10.1016/0009-2541(94)00140-4

Metcalf, R. V., & Shervais, J. W. (2008). Suprasubduction-zone ophiolites: Is there really an ophiolite conundrum? In: Wright, J. E., & Shervais, J. W. (Eds.). *Ophiolites, Arcs, and Batholiths: A Tribute to Cliff Hopson.* Geological Society of America Special Papers, 438(January), 191–222. https://doi.org/10.1130/2008.2438(07)

Miyashiro, A. (1973). The Troodos ophiolitic complex was probably formed in an island arc. *Earth and Planetary Science Letters,* 19(2), 218–224. https://doi.org/https://doi.org/10.1016/0012-821X(73)90118-0

Moreno, A. (2017). *Estudio Petrogenético de las Rocas Gabroideas del Complejo Ofiolítico de Ginebra, Valle del Cauca.* Universidad Nacional de Colombia.

Nelson, H. W (1957). Contribution to the geology of the Central and Western Cordillera of Colombia in the sector between Ibague and Cali. *Leidse Geologische Medelelingen*, 22, 1-76.

Nivia, A. (1987). G*eochemistry and origin of the Anaime and volcanic sequences South western Colombia.* [Unpublished M. Phil. Thesis, University of Leicester, UK.]

Nivia, Á. (1994). The Bolivar mafic–ultramafic complex, SW Colombia: the base of an obducted oceanic plateau. *Journal of South American Earth Sciences*, 9(1-2), 59-68. https://doi.org/10.1016/0895-9811(96)00027-2

Nivia, Á. (2001). Mapa Geológico del Valle del Cauca "Memoria Explicativa". *Ingeominas,* 148. http://recordcenter.sgc.gov.co/B4/13010040024334/documento/pdf/0101243341101000.pdf

Nivia, A., Tarazona, C., & Paz, D. (2017). *Geología y geocronología del Batolito de Buga y el Macizo Ofiolítico de Ginebra, Colombia.* Memorias, XVI Congreso Colombiano de Geología. Santa Marta. August.

Nivia, A., Tarazona, C., & Paz, D. (2019). *Petrogénesis y edad de las rocas ultramáficas y máficas del complejo ultramáfico de Venus, el macizo ofiolítico de Ginebra y su relación con el Batolito de Buga, Valle del Vauca.* Memorias, XVII Congreso Colombiano de Geología. Santa Marta. August.

Ossa Meza, C., & Concha Perdomo, A. (2007). Petrogénesis de las rocas del Macizo Ofiolítico de Ginebra entre las veredas La Honda (Ginebra) y El Diamante (Buga) en el departamento del Valle del Cauca. *Geología Colombiana*, 32, 97–110.

Ozkan, M., Celik, O. F., Soycan, H., Cortuk, R. M., & Marzoli, A. (2020). The Middle Jurassic and Early Cretaceous basalt-radiolarian chert association from the Tekelidağ Mélange, eastern İzmir-Ankara-Erzincan suture zone (northern Turkey). *Cretaceous Research*, *107*, 104280.

Pearce, J. (1982). *Trace element characteristics of lavas from destructive plate boundaries*. (Ed. RS Thorpe). Orogenic andesites and related rocks, Chichester, England: John Wiley and Sons, pp. 528-548.

Pearce, J. A., Lippard, S. J., & Roberts, S. (1984). Characteristics and tectonic significance of supra-subduction zone ophiolites. *Geological Society Special Publication*, 16, 77–94. https://doi.org/10.1144/GSL.SP.1984.016.01.06

Pearce, J. A., & Peate, D. W. (1995). Tectonic implications of the composition of volcanic arc magmas. *Annual review of Earth and planetary sciences*, *23*, 251-286. https://doi.org/10.1146/annurev.ea.23.050195.001343

Pearce, J. A. (2008). Geochemical fingerprinting of oceanic basalts with applications to ophiolite classification and the search for Archean oceanic crust. *Lithos*, *100*(1-4), 14-48. https://doi.org/10.1016/j.lithos.2007.06.016

Pearce, J. A. (2014). Immobile Element Fingerprinting of Ophiolites. *Elements,* 10(2), 101–108. https://doi.org/10.2113/gselements.10.2.101

Peccerillo, A. & Taylor, S. R. (1976). Geochemistry of Eocene calc-alkaline volcanic rocks from the Kastamonu area, Northern Turkey. Contributions to Mineralogy and Petrology 58, 63–81.

Proenza, J. A., Ortega-Gutiérrez, F., Camprubı, A., Tritlla, J., Elıas-Herrera, M., & Reyes-Salas, M. (2004). Paleozoic serpentinite-enclosed chromitites from Tehuitzingo (Acatlán Complex, southern Mexico): a petrological and mineralogical study. *Journal of South American Earth Sciences*, *16*(8), 649-666. https://doi.org/10.1016/j.jsames.2003.12.003

Restrepo, A., & Julián, J. (2008). Obducción y metamorfismo de ofiolitas triásicas en el flanco occidental del terreno Tahamí, cordillera central de Colombia. *Boletín de Ciencias de la Tierra,* 22, 49-100.

Rodríguez, B. P. (2012). *Estudio metalogenético de las mineralizaciones auríferas del área de Ginebra y zonas aledañas, Valle del Cauca.* Universidad Nacional de Colombia. https://repositorio.unal.edu.co/handle/unal/21336

Schwinn, W. L. (1969). *Guidebook to the geology of the Cali area*. Colombian Society of Petroleum Geologist and Geophysicist, 10th field trip, 29 p. Bogotá.

Shand, S. J. (1943). Classic A/CNK vs A/NK plot for discriminating metaluminous, peraluminous and peralkaline compositions.

Toussaint, J. F., & Restrepo, J. J. (1978). Edad K/Ar de dos rocas básicas del flanco noroccidental de la cordillera central. Boletín de Ciencias de la Tierra, (5-6), 71-72.

Van Der Hammen, T. (1958). Estratigrafía del Terciario y Maestrichtiano continentales y tectogénesis de los Andes Colombianos. *Boletín Geológico* 6(1-3), 60-116.

Villagómez, D., Spikings, R., Magna, T., Kammer, A., Winkler, W., & Beltrán, A. (2011). Geochronology, geochemistry and tectonic evolution of the Western and Central cordilleras of Colombia. *Lithos,* 125(3–4), 875–896. https://doi.org/10.1016/j.lithos.2011.05.003

Yang, G., Li, Y., Safonova, I., Yi, S., Tong, L., & Seltmann, R. (2014). Early Carboniferous volcanic rocks of West Junggar in the western Central Asian Orogenic Belt: implications for a supra-subduction system. *International Geology Review*, 56(7), 823–844. https://doi.org/10.1080/00206814.2014.902757

ANNEX 1

Information on thin-sections analyzed

ID	Coordinates*		Classification	Mineralogy
	East	North		
DEG190423Aa	1097436	906969	Diorite	Pl, Cpx, Qz, Ep, Czo, Zrn, Spn, Rt, Amp, Mgt
DEG190423Ab	1097436	906969	Gabbrodiorite	Pl, Cpx, Mgt, Amp, Ilm, Py, Ccp, Ep
DEG190423Ac	1097436	906969	Diorite	Pl, Cpx, Qz, Czo, Ilm, Ep, Amp, Opx, Py, Ilm, Hem, Spn
DEG190423Ba	1097370	906975	Gabbrodiorite	Pl, Cpx, Amp, Opx, Ep, Chl, Mgt, Ilm, Py, Hem, Zrn
DEG190423Bb	1097370	906975	Gabbrodiorite	Pl, Cpx, Ilm, Qz, Mgt, Ep, Opx
DEG190424Ab	1097687	906597	Gabbro	Pl, Amp, Cpx, Ep, Mgt, Ser
DEG190424Ac	1097687	906597	Gabbro	Cpx, Pl, Amp, Zo, Czo, Ilm, Chl

*Datum-Origen: MAGNA-Bogota Oeste

Amp: amphibole; Ccp: chalcopyrite; Chl: chlorite group; Cpx: clinopyroxene; Czo: clinozoisite, Ep: epidote, Hem: hematite; Ilm: ilmenite; Mgt: magnetite, Opx: orthopyroxene; Pl: plagioclase; Py: pyrite; Qz: quartz; Rt: rutile; Ser: sericite; Spn: sphene, Zrn: zircon.

ANNEX 2

Calibrations standards for the ICP-AES and ICP-MS analysis and detection limits for every analyzed element

Method	Analyzed Elements (Detection limits)	Standards (Elements)	Unities
ICP-AES	Al_2O_3 (0,01-100), BaO (0,01-100), CaO (0,01-100), CrO_3 (0,01-100), Fe_2O_3 (0,01-100), K_2O (0,01-100), MgO (0,01-100), MnO (0,01-100), Na_2O (0,01-100), P_2O_5 (0,01-100), SiO_2 (0,01-100), SrO (0,01-100), TiO_2 (0,01-100), LOI (0,01-100).	**NCS 14015b, NCSDC71301, NCSDC73303, SARM-12, OREAS 24b** (Al_2O_3, BaO, CaO, CrO_3, Fe_2O_3, K_2O, MgO, MnO, Na_2O, P_2O_5, SiO_2, SrO, TiO_2, LOI)	Percentage (%)
ICP-MS	Ba (0,5-10000), Ce (0,1-10000), Cr (10-10000), Cs (0,01-10000), Dy (0,05-1000), Er (0,03-1000), Eu (0,03-1000), Ga (0,1-1000), Ge (5-1000), Gd (0,05-1000), Hf (0,2-10000), Ho (0,01-10000), La (0,1-10000), Lu (0,01-1000), Nb (0,2-2500), Nd (0,1-10000), Pr (0,03-1000), Rb (0,2-10000), Sm (0,03-10000), Sn (1-10000), Sr (0,1-10000), Ta (0,1-2500), Tb (0,01-1000), Th (0,05-1000), Tm (0,1-1000), U (0,05-1000), V (5-10000), W (1-10000), Y (0,1-10000), Yb (0,03-1000), Zr (2-10000).	**GRE-3, OREAS 24b** (Ba, Ce, Cr, Cs, Dy, Er, Eu, Ga, Gd, Ge, Hf, Ho, La, Lu, Nb, Nd, Pr, Rb, Sm, Sn, Sr, Ta, Tb, Th, Tm, U, V, W, Y, Yb, Zr) **MRGeo08, GBM908-10** (Ag, Cd, Co, Cu, Li, Mo, Ni, Pb, Sc, Zn, As, Bi, Hg, In, Re, Sb, Sc, Se, Te, Tl)	Parts-per million (ppm)

ANNEX 3

Table 1. Total rock chemical analysis in major and trace elements of GOC rocks in the Puente de Piedra section.

Oxide (%)	DEG190423Aa	DEG190423Ab	DEG190423Ac	DEG190423Ba	DEG190423Bb	DEG190424Ab	DEG190424Ac
SiO_2	57,29	58,98	60,99	52,98	54,09	49,56	50,34
Al_2O_3	13,72	12,82	12,2	11,96	13,96	16,78	14,88
Fe_2O_3	8	14,34	5,3	6,42	9,66	8,86	7,24
MgO	5,36	2,75	5,24	10,35	7,38	6,9	8,71
CaO	12,05	8,17	12,2	15,85	12,7	14,8	15,25
Na_2O	3	3,17	3,11	2,04	3,11	2	1,9

Oxide (%)	DEG190423Aa	DEG190423Ab	DEG190423Ac	DEG190423Ba	DEG190423Bb	DEG190424Ab	DEG190424Ac
K_2O	0,03	0,03	0,03	0,05	0,04	0,05	0,06
TiO_2	0,52	0,74	0,87	0,13	0,23	0,4	0,57
P_2O_5	<0.01	0,08	0,01	<0.01	0,01	0,01	<0.01
MnO	0,15	0,14	0,13	0,15	0,13	0,15	0,14
Cr_2O_3	0,01	0,01	<0.01	0,01	0,01	0,06	0,07
LOI	0,82	-0,06	0,26	0,86	0,12	1,84	1,03
Total	101,15	101,45	100,65	101,1	101,75	101,7	100,45
Element (ppm)							
Ba	10,3	12	15,5	16,2	31,2	13,2	11,7
Co	24	29	21	30	32	26	27
Cs	<0.01	0,03	0,02	0,07	0,02	<0.01	0,03
Ga	13	14,9	14	8	11,3	13,8	13,5
Hf	0,6	1,3	1,4	0,3	0,4	0,8	0,9
Nb	2,3	1,6	4,9	<0.2	7	0,7	1,3
Rb	0,5	0,3	0,8	1,1	0,6	1,1	1,2
Sn	1	1	1	1	1	1	1
Sr	98,2	79,3	84,8	64,8	68,5	105	83,8
Ta	0,1	0,2	0,2	0,1	0,5	0,1	0,2
Th	0,2	0,17	0,36	0,08	0,32	0,21	0,15
U	0,09	0,06	0,11	<0.05	0,24	<0.05	<0.05
V	277	252	180	129	229	252	228
W	<1	1	1	1	1	1	<1
Zr	20	38	40	11	15	26	29
Y	33,7	23,4	32,5	12,5	10,4	8,5	13,5
La	2	1,8	2,3	0,8	5	1,2	1,1
Ce	8	4,8	8,9	2,5	10,3	2,6	2,7
Pr	1,64	0,89	1,77	0,49	1,33	0,41	0,49
Nd	9,2	4,7	10,6	2,9	5,5	2,2	2,5
Sm	3,11	1,67	3,84	1,04	1,29	0,8	0,95
Eu	0,89	0,65	0,95	0,38	0,4	0,34	0,41
Gd	4,65	2,68	4,96	1,81	1,67	1,19	1,66
Tb	0,78	0,53	0,86	0,31	0,25	0,25	0,3
Dy	5,87	3,82	5,66	2,12	1,87	1,4	2,4
Ho	1,15	0,81	1,19	0,43	0,35	0,28	0,45
Er	3,96	2,88	3,7	1,37	1,16	1,02	1,35
Tm	0,54	0,38	0,56	0,22	0,17	0,14	0,24
Yb	3,9	2,87	3,65	1,28	1,25	1	1,5

Oxide (%)	DEG190423Aa	DEG190423Ab	DEG190423Ac	DEG190423Ba	DEG190423Bb	DEG190424Ab	DEG190424Ac
Lu	0,56	0,47	0,56	0,2	0,19	0,13	0,18
Mo	1	2	<1	1	1	1	1
Cu	6	3	21	13	5	13	17
Pb	<2	3	<2	<2	<2	<2	<2
Zn	27	42	21	30	27	38	33
Ni	44	14	66	79	49	64	106
Cr	120	30	10	110	50	440	550
As	0,2	0,1	0,2	0,2	0,1	<0.1	0,3
Cd	<0.5	<0.5	<0.5	<0.5	<0.5	0,5	<0.5
Sb	<0.05	<0.05	<0.05	<0.05	<0.05	<0.05	<0.05
Bi	<0.01	<0.01	0,07	<0.01	0,03	<0.01	0,01
Ag	<0.5	<0.5	<0.5	1,4	<0.5	<0.5	<0.5
Hg	<0.005	<0.005	<0.005	<0.005	<0.005	0,007	<0.005
Tl	<0.02	<0.02	<0.02	<0.02	<0.02	<0.02	<0.02
Se	0,3	<0.2	<0.2	<0.2	<0.2	<0.2	<0.2
Li	<10	<10	<10	10	10	<10	<10
Sc	42	38	35	63	52	39	43
In	0,009	0,015	0,005	0,005	<0.005	<0.005	<0.005
Re	<0.001	0,001	<0.001	<0.001	<0.001	<0.001	<0.001
Sc	3,7	3,7	2,5	4,9	2,7	2,6	2,3
Te	0,01	0,02	<0.01	0,01	0,01	0,01	<0.01
S	0,01	<0.01	0,02	0,01	0,01	0,01	0,01
C	0,03	0,13	0,03	0,06	0,04	0,17	0,05
Ge	<5	<5	<5	<5	<5	<5	<5

Table 2. The CIPW norm for the GOC rocks minerals in the Puente Piedra section.

% weight							
CIPW Norm	DEG190423Aa	DEG190423Ab	DEG190423Ac	DEG190423Ba	DEG190423Bb	DEG190424Ab	DEG190424Ac
Quartz	13,68	23,21	17,76	3,48	6,06	3,67	2,86
Zircon		0,01				0,01	
Anorthite	23,88	20,66	19,24	23,33	24,01	36,66	31,90
Diopside	26,93	13,47	28,15	43,02	30,07	27,87	32,80
Sphene	0,89	1,46	1,81		0,22	0,65	1,12
Hypersthene	0,87	0,61		5,84	4,44	4,27	6,49
Albite	25,39	26,82	26,32	17,26	26,32	16,92	16,08
Orthoclase	0,18	0,18	0,18	0,30	0,24	0,30	0,35
Wollastonite			1,05				
Apatite	0,02	0,19	0,02	0,02	0,02	0,02	0,02
Pyrite	0,02	0,02	0,04	0,02	0,02	0,02	0,02
Chromite	0,03			0,03	0,01	0,09	0,12
Ilmenite	0,30	0,28	0,25	0,25	0,26	0,26	0,22

% weight							
CIPW Norm	**DEG190423Aa**	**DEG190423Ab**	**DEG190423Ac**	**DEG190423Ba**	**DEG190423Bb**	**DEG190424Ab**	**DEG190424Ac**
Magnetite				0,08			
Hematite	8,00	14,34	5,30	6,37	9,66	8,86	7,24
Quartz	15,15	25,61	19,43	3,99	6,76	4,18	3,28
Zircon		0,01				0,01	
Anorthite	25,40	21,89	20,21	25,66	25,72	40,02	35,13
Diopside	24,55	12,23	25,35	40,55	27,62	26,08	30,96
Sphene	0,75	1,22	1,50		0,19	0,56	0,97
Hypersthene	0,79	0,55		5,52	4,09	4,01	6,15
Albite	28,44	29,94	29,12	20,00	29,70	19,46	18,65
Orthoclase	0,20	0,20	0,20	0,35	0,27	0,35	0,42
Wollastonite			1,06				
Apatite	0,02	0,17	0,02	0,02	0,02	0,02	0,02
Pyrite	0,01	0,01	0,02	0,01	0,01	0,01	0,01
Chromite	0,02			0,02	0,01	0,05	0,07
Ilmenite	0,18	0,17	0,15	0,16	0,16	0,16	0,14
Magnetite				0,05			
Hematite	4,47	7,99	2,93	3,68	5,44	5,09	4,19